

Flexible Technologies for Self-Powered Wearable Health and Environmental Sensing

This article addresses the key challenges in wearable health and environmental systems that enable ultra-long battery lifetime, user comfort and wearability.

By VEENA MISRA, *Fellow IEEE*, ALPER BOZKURT, BENTON CALHOUN, THOMAS JACKSON, JESSE S. JUR, JOHN LACH, *Senior Member IEEE*, BONGMOOK LEE, JOHN MUTH, ÖMER ORALKAN, *Senior Member IEEE*, MEHMET ÖZTÜRK, *Fellow IEEE*, SUSAN TROLIER-MCKINSTRY, *Fellow IEEE*, DARYOOSH VASHAEE, DAVID WENTZLOFF, AND YONG ZHU

ABSTRACT | This article provides the latest advances from the NSF Advanced Self-powered Systems of Integrated sensors and Technologies (ASSIST) center. The work in the center addresses the key challenges in wearable health and environmental systems by exploring technologies that enable ultra-long battery lifetime, user comfort and wearability, robust medically validated sensor data with value added from multimodal sensing, and access to open architecture data streams. The vision of the ASSIST center is to use nanotechnology to build miniature, self-powered, wearable, and wireless sensing devices that can enable monitoring of personal health and personal environmental exposure and enable correlation of multimodal sensors. These devices can empower patients and doctors to transition from

managing illness to managing wellness and create a paradigm shift in improving healthcare outcomes. This article presents the latest advances in high-efficiency nanostructured energy harvesters and storage capacitors, new sensing modalities that consume less power, low power computation, and communication strategies, and novel flexible materials that provide form, function, and comfort. These technologies span a spatial scale ranging from underlying materials at the nanoscale to body worn structures, and the challenge is to integrate them into a unified device designed to revolutionize wearable health applications.

KEYWORDS | Atomic layer deposition; CMUT; environmental monitoring; environmental sensor; flexible electrode; motion harvesting; physiological sensor; piezoelectric; PZT; self-powered; silver nanowire; TEG; thermoelectrics; ultra-low power; ultra-low power SOC; volatile organic compound sensor; wearable device

Manuscript received November 19, 2014; revised January 25, 2015 and February 25, 2015; accepted March 3, 2015. Date of current version May 19, 2015. This work was funded by National Science Foundation Nanoscience Engineering Research Center for Advanced Self-Powered Systems of Integrated Sensors and Technologies (EEC-1160483).

V. Misra, A. Bozkurt, J. Muth, Ö. Oralkan, and M. Öztürk are with the Electrical and Computer Engineering Department, North Carolina State University, Raleigh, NC 27695 USA.

B. Calhoun and J. Lach are with the Electrical and Computer Engineering Department, University of Virginia, Charlottesville, VA 22904 USA.

T. Jackson is with the Electrical and Computer Engineering Department, Pennsylvania State University, State College, PA 16801 USA.

J. Jur is with the Department of Textile Engineering, Chemistry and Science, North Carolina State University, Raleigh, NC 27695 USA.

B. Lee and D. Vashae are with the Electrical and Computer Engineering Department, North Carolina State University, Raleigh, NC 27695 USA.

S. Trolrier-Mckinstry is with the Materials Science and Engineering Department, Pennsylvania State University, University Park, PA 16801 USA.

D. Wentzloff is with the Electrical Engineering and Computer Science Department, University of Michigan, Ann Arbor, MI 48109 USA.

Y. Zhu is with the Mechanical and Aerospace Engineering Department, North Carolina State University, Raleigh, NC 27695 USA.

Digital Object Identifier: 10.1109/JPROC.2015.2412493

0018-9219 © 2015 IEEE. Personal use is permitted, but republication/redistribution requires IEEE permission. See http://www.ieee.org/publications_standards/publications/rights/index.html for more information.

I. INTRODUCTION

Wearable systems represent an unusual intersection of engineering, design, and fashion. While their function promises a compelling future of personal health and environmental monitoring, their form and usability—especially their comfort and system battery lifetime—will be at least as important for ensuring user adoption. Advances in embedded sensors, processing units, wireless transceivers, and energy supplies have yielded the wristbands, chest patches, chest bands, eyeglasses, headsets,

etc. that have launched the “quantified self” movement, with FDA-approved devices emerging for numerous medical applications. But additional innovations in flexible, ultra-low-power technologies are necessary to provide greater functional capabilities for new health applications while improving comfort and system battery lifetimes. In fact, it has recently been reported that the effectiveness of currently available wearable devices is not ideal, due primarily to their limitations in comfort and power consumption (requiring frequent charging) [1]. This indirectly reduces compliance and prevents the inclusion of additional sensing modalities that would only add to comfort and power concerns, especially when extending such systems to users beyond healthy ‘quantified selfers’ to children, the elderly, and those with chronic diseases.

The vision of the NSF funded Engineering Research Center for Advanced Self-Powered Systems of Integrated Sensors and Technologies (ASSIST) is to use nanotechnology to build flexible, self-powered, multimodal wearable sensing devices that can enable monitoring of personal health and environmental exposure with maximum comfort and system lifetime. Fig. 1 shows the critical components of a self-powered wearable platform. These include energy harvesting, energy storage, physiological and environmental sensors, computation and communication units, and flexible materials for integrating these technologies into novel form factors. The ASSIST Center is developing core technologies that target maximizing the power harvested from the body in the form of *heat and movement/strain using flexible materials* while simultaneously minimizing the power consumption via *subthreshold CMOS computation and ultra low-power radios*, thus shifting the balance in Fig. 2 such that the system never needs to be recharged from a wall socket. In addition, ASSIST is building ultra low-power health sensors (EKG, hydration, pulse-oximetry, biochemical markers such as cortisol or amylase) and environmental exposure sensors (gases and particulate matter) that go much further than simple activity monitoring and provide a significantly more

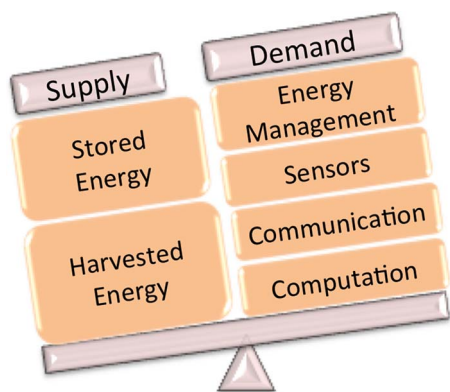


Fig. 1. Critical components of a self-powered wearable sensor platform.

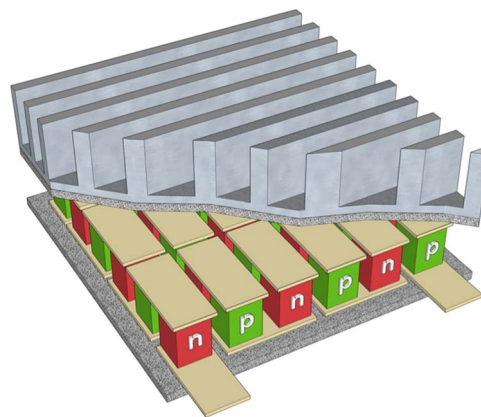


Fig. 2. A typical TEG consisting of semiconductor legs between two thermally rigid substrates.

sophisticated understanding of human health with correlation of heterogeneous data streams (Section IV). This combination of **flexible materials** (energy harvesting and sensors), a **positive power balance** [energy harvesting (Section II) and ultra low-power sensing, computation, and communication (Section III)], and **heterogeneous sensing modalities** enables *comfortable forever—and therefore user-compliant—operation* of wearable sensor systems for longitudinal health monitoring of diverse user groups and assists in creating a paradigm shift towards personalized medicine and wellness management.

II. FLEXIBLE ENERGY HARVESTING

Powering of flexible wearable electronics requires a multitude of approaches from researching new materials for smaller, faster charging and more energy efficient batteries to improving the efficiency of existing energy storage devices such as lithium ion cells and supercapacitors. It is important that better power management through dynamic voltage scaling, optimal system energy management techniques are used through more efficient sensors, processors and algorithms. While there are many available sources of energy from the body and environment, the ASSIST Center is focused on autonomous sources of power, namely, body heat and body motion. These harvesting technologies are discussed below.

A. Body Heat

Thermoelectric energy generators (TEGs) placed on the body can convert the temperature differential, ΔT , between the skin and the ambient into a voltage, $\Delta V = -\alpha\Delta T$. The proportionality constant, is known as the Seebeck coefficient and is property of the thermoelectric material. A typical TEG is constructed by sandwiching a series of semiconductor legs between two thermally conductive rigid substrates as shown in Fig. 2. Because the polarity of the Seebeck coefficient is opposite for p- and

n-type legs, by connecting the alternately doped legs electrically in series, the Seebeck voltages produced by the legs can be added to obtain a larger voltage. The electrical resistances of the legs also add up, establishing the output resistance of the generator. Finally, to maintain a large ΔT , materials with low thermal conductivity are needed. The Seebeck coefficient, α , the electrical conductivity, σ , and the thermal conductivity, κ , are combined in a dimensionless figure-of-merit ZT given by

$$ZT = \frac{\sigma\alpha^2}{\kappa} T \quad (1)$$

where T is the ambient temperature in Kelvin. Commercial TEGs operate with ZT values within 0.7 to 1 and significant research efforts are underway to improve ZT .

The grand challenge in using TEGs on the human body is obtaining a large ΔT across the device in order to maximize the output voltage and power. Unfortunately, the parasitic thermal resistances at the TEG/ambient and skin/TEG interfaces can significantly reduce the resulting ΔT across the device to only $\sim 1-2$ °C which can in turn decrease the output power of TEGs by orders of magnitude. Since the parasitic resistance at the TEG/ambient interface is dominated by the convection resistance a heatsink is typically attached to the TEG's cold-side to increase the surface area for more effective cooling via convection. Ideally, the use of a large heatsink can minimize this resistance however the total form factor and user comfort level will limit the heatsink size. The second parasitic thermal resistance is introduced by the skin and the contact resistance at the TEG/skin interface. Achieving a good thermal contact between the TEG and the skin is difficult with rigid TEGs unless pressure is applied to flatten the skin. Furthermore, it is unlikely that a single small TEG will be capable of delivering the desired power levels needed by future sensors and electronics with power demands reaching milliwatts (mW). Therefore, a TEG band will most likely be needed for advanced wearables powered by TEGs. A potential solution is to integrate many small rigid TEGs into a flexible band, which brings its own manufacturing challenges and while also increasing cost. A single, large-area flexible harvester can address both challenges.

To date many attempts have been made to create flexible thermoelectric harvesters. Some of these attempts rely on thin-film deposition techniques (e.g., evaporation, sputtering and more recently, printing) to deposit thermoelectric materials on flexible substrates (e.g., polyimide). Unfortunately, these harvesters are well behind the performance levels of the best rigid harvesters because the designs often require compromises in properties of the thermoelectric and packaging materials as well as the dimensions of the thermoelectric legs. Among the more successful examples, a flexible harvester by Glatz *et al.* [2] was able to reach $25 \mu\text{W}/\text{cm}^2$ with a temperature differential of 10 °C. The TEG legs in their device were formed by pulsed electrochemical deposition. More

recently, Kim *et al.* [3] achieved $100 \mu\text{W}/\text{cm}^2$ for the same temperature differential with a device featuring a glass fabric and screen-printed thermoelectric legs embedded in PDMS. While both approaches yielded higher performance figures than those achieved with previous flexible harvesters, their performance is still well behind those of the best rigid devices. More importantly, thermoelectric harvesters operating on the human body must perform with temperature differentials on the order of 1 °C further reducing the abovementioned power levels down to a few microwatts. In ASSIST, we are targeting power levels as high as 500 μW to power multiple sensors and electronics planned on our wearables.

In ASSIST, a new approach is being sought to produce flexible TEGs. The approach relies on developing flexible packages that can be populated using pick-and-place equipment similar to those used by standard rigid TEGs. The goal is to develop a package compatible with any TEG material including those developed in ASSIST as long as standard assembly techniques can be employed. An example half-package is shown in Fig. 3, which shows TEG legs bonded to a flexible polyimide substrate with thru holes filled with copper. The copper vias provide the metallic base for thermal compression bonding of the TEG legs. The vias also thermally shunt the polyimide substrate resulting in a very small thermal resistance between the heat source and the TEG legs. The approach can enable manufacturing of flexible TEGs with performance levels comparable to or better than the rigid TEGs by eliminating the traditional compromises made in flexible devices (e.g., the thermoelectric material quality, and parasitic thermal resistances introduced by the flexible materials.)

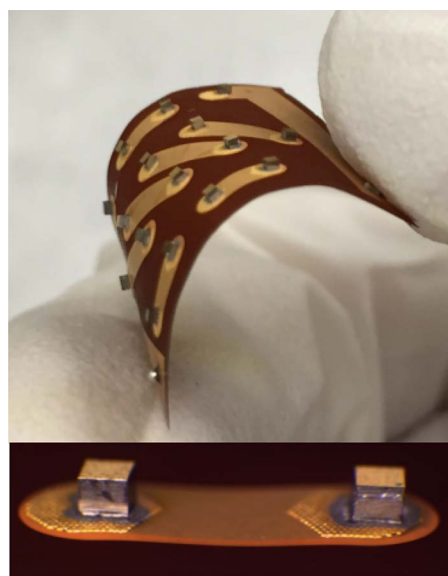


Fig. 3. Optical image of flexible package. TEG legs are bonded to Cu pillars obtained by filling the through holes formed in the photodefinable polyimide, HD-4110.

Considerable effort is also being dedicated to modeling of the TEG operation on the human body not only to optimize the flexible TEG package but also to choose the most suitable semiconductor parameters for this specific application. Fig. 4 shows the results for the maximum possible output power of a $1\text{ cm} \times 1\text{ cm}$ TEG as a function of the thermal conductivity of the semiconductor legs. Different ZT values have been obtained by adjusting the electrical conductivity of the material while keeping the Seebeck coefficient constant at $200\text{ }\Delta V/K$. It can be seen that for a given thermal conductivity, improving the ZT figure-of-merit certainly improves the output power. However, more interestingly, it is seen that the output power increases more rapidly with decreasing the thermal conductivity than increasing the ZT . In fact, a thermoelectric material with a low thermal conductivity $< 0.4\text{ W/mK}$, (even with a poor ZT of 0.5) can perform better than a material with a high ZT of 2 but thermal conductivity higher than 1 W/mK . The need for semiconductors with the lowest possible thermal conductivity is due to the large parasitic thermal resistances that exist at the skin/TEG and TEG/air interfaces. These resistances make it extremely challenging to achieve a large enough across the device. In ASSIST, we are exploring nanocomposites of $(\text{Bi}, \text{Sb})_2(\text{Se}, \text{Te})_3$ based materials for a higher performance TEG operation on the human body. A key advantage of such nanocomposites is their ability to reduce the thermal conductivity of the material. This is achieved by phonon scattering at the grain boundaries resulting in very small thermal conductivity values appropriate for body heat energy harvesting applications. Fig. 5 shows a transmission electron microscope (TEM) image of the interface of several grains in nanocomposite bulk sample. The sizes of these grains are typically smaller than the mean free path of the majority of phonons but larger than

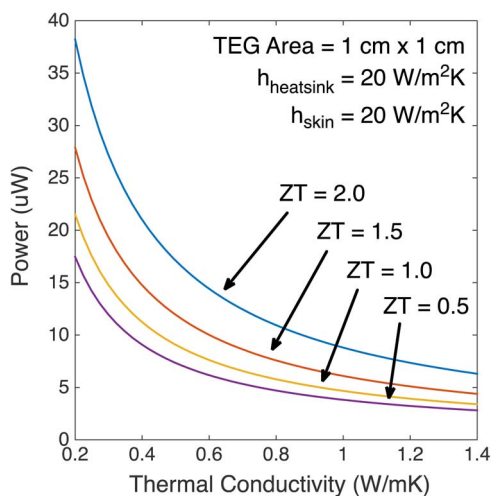


Fig. 4. Maximum output power of a TEG calculated as a function of the thermal conductivity of the semiconductor legs with different ZT values.

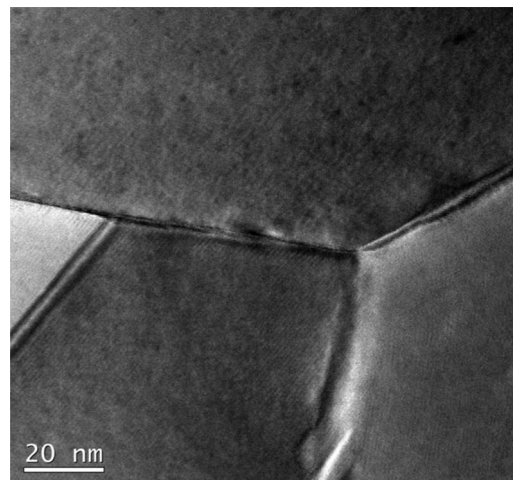


Fig. 5. Transmission electron microscopy image of the grain boundaries in $(\text{Bi}, \text{Sb})_2\text{Te}_3$ based nanocomposites being explored in ASSIST for high-performance TEG operation on human body.

the mean free path of the charge carriers. Therefore, the reduction in thermal conductivity often happens without significant deterioration of the electrical conductivity.

Electrons and phonons in nanocomposites experience several transport processes that do not occur in other thermoelectric or electronic materials. Phonon scattering at grain boundaries, dopant diffusion and precipitation, reduced bipolar thermal diffusion of electron-hole pairs, electron transitions through the same and different valleys at grain boundaries, thermionic emission at grain boundaries, and partial relaxation of the carrier energy at nanoscale grains are some of the main mechanisms that can significantly affect the thermoelectric properties of nanocomposites [4]. Therefore, with further engineering of the grain size, alloy composition ratios, carrier concentration, grain boundary potential, etc., we can further optimize the thermoelectric properties according to the application requirements.

B. Body Motion

There have been a large number of publications describing scavenging of mechanical energy from vibrational motion [5]–[7]. For unobtrusive systems, one of the challenges is either to make the device small, or to incorporate the harvester into clothing. In considering different approaches to scavenging mechanical energies, it has been reported that when electromagnetic dynamos are scaled to small dimensions (e.g., sub cm) then the output voltage may become too low for use [5]. While electrostatic generators perform well in MEMS scale devices, they require a priming charge from a power supply which may not be available for many applications. Piezoelectrics however, can output electric energy at several volts and have a high energy density, making them feasible for MEMS energy harvesters [6].

The key challenge in scavenging motion from the human body is the fact that the body does not move

periodically [7]. Furthermore, except at joints, the amplitudes of the accelerations/strains tend to be modest. While linear oscillators are well suited to harvest vibrations very close to their natural frequency, they collect little of the vibration energy existing outside this narrow band. Thus, practical designs for scavenging energy from human motion often either utilize the large stresses (strains) associated with heel strikes or joint motion, or utilize nonlinear harvesters which more efficiently scavenge energies from a broader frequency range [8], [9].

Thus, the goal for motion harvesting is to increase the scavenged energy from mechanical motion by utilizing a combination of good mechanical design which couples the energy from the moving body into a piezoelectric material, efficient transduction from mechanical to electrical energies through the use of piezoelectric films with high energy harvesting figures of merit, and efficient extraction of energy via an electrical circuit. This is shown schematically in Fig. 6. In its simplest embodiment, many mechanical harvesters are end-loaded cantilevers for which the resonance frequency has been tuned to match motion of the structure. Substantially higher outputs can be achieved if all parts of the system can be simultaneously optimized, as is being done in the ASSIST Center.

Several approaches are being utilized to increase the scavenged energy from body motion. One of the approaches is the development of low-frequency, comparatively broadband resonant scavengers. Fig. 6 shows schematically a hinged design in which a piezoelectric material (the middle of the three “fingers” in the structure) is bent into an approximately parabolic geometry by a body acceleration. This strains the piezoelectric material far more uniformly than can be done in an end-loaded cantilever, increasing the energy output. In addition, through appropriate design of the hinges and end mass, devices with resonant frequencies can be made from 7 to 10 Hz.

ASSIST has also considerably increased the figure of merit for conversion of mechanical energy to electrical

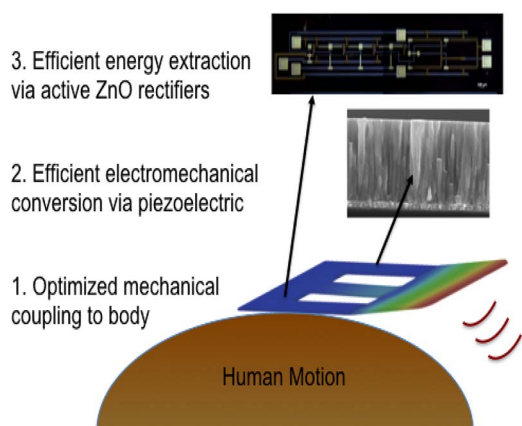


Fig. 6. System-level issues in mechanical energy harvesting.

energy through the deposition of domain-controlled piezoelectric films onto flexible metal foils [10]–[12]. Fundamentally, this entails deposition of $\text{PbZr}_{0.52}\text{Ti}_{0.48}\text{O}_3$ (PZT) films onto metal foils with larger thermal expansion coefficients. In this way, the ferroelectric polarization can be forced out of the plane of the film, increasing the piezoelectric coefficient, and decreasing the dielectric permittivity. This increases the energy harvesting figure of merit by a factor of 2–6 relative to PZT films on Si substrates. Moreover, the metal substrates also provide substantially improved mechanical reliability than brittle passive elastic layers such as Si, silicon nitride, etc.

The films are readily machined into a wide variety of harvester geometries, including the hinged design described above, as well as for joint-based harvesters. An example of this is shown in Fig. 7, which shows a piezoelectric PZT film on a nickel (Ni) foil used to scavenge energy from motion of a human elbow. In the figure, a PZT film on Ni is encapsulated in kapton tape (the slightly orange colored material visible as a thin layer near the elbow). When the elbow is bent, as can be seen in the left-hand portion of the figure, the device is stretched. When the elbow is straightened, the distance between the attachment points is reduced, and the harvester buckles away from the elbow. This strains the PZT, and produces power for each motion of the elbow.

The third critical function of a mechanical harvester is to efficiently extract the electrical energy from the piezoelectric, rectify it, and store it for later use. Most piezoelectric devices output AC electrical signals. These must be rectified to enable storage in a battery or supercapacitor. Many rectifiers use diodes with a comparatively high voltage for “turn-on.” Low voltages (~ 0.2 – 0.3 V) produced by



Fig. 7. Piezoelectric-coated film on a Ni foil, bent around an elbow.

the piezoelectric that do not reach this threshold represent power that is “lost” from the system. Thus, in order to extract the maximum power from the harvester, it is useful to be able to tune the voltage of the diode to near zero volts, and to be able to rapidly switch between the two polarities, so that the majority of the electrical energy can be saved. Thus, the tactic being taken here is to fabricate electronics directly on the mechanical energy harvesting system, to enable rapid switching and detection of the zero crossing points on the harvester output. Furthermore, we anticipate that building the electronics directly on the harvester will be advantageous in power matching and power combining.

For this purpose, ZnO thin film transistors (TFTs) are being utilized. Plasma-enhanced atomic layer deposition of the ZnO semiconductor and Al₂O₃ dielectric layers enables circuit fabrication at < 200 °C, and does not degrade the piezoelectric, so that the electronics can, in principle, be built directly on the mechanical energy harvester. The necessary components are stable TFTs and a route to high gain amplifiers. The voltage delivered by a piezoelectric energy harvester is often small and conventional rectification schemes (diodes) lead to significant energy loss. Power matching and power combining is also problematic. Integrated electronics will significantly increase the available energy output from these energy harvesters. Co-integration of ZnO TFT and PZT microelectromechanical systems has been demonstrated in ASSIST without degrading the performance of either component. Furthermore, double gate ZnO TFTs that can be used in an enhancement/depletion configuration to provide gain > 100 in a simple inverter have also been demonstrated [13]. This is a key result to allow low-voltage, TFT-based rectification for piezoelectric energy harvesters. To circumvent the difficulties associated with the large knee voltages of standard diodes (~0.3 V), active rectification was pursued for the mechanical energy harvesters. Double gate ZnO TFT's with ZnO layer thicknesses in the range of 10–50 nm were designed for this purpose. This allows us to use the top gate to tune the active rectifier turn-on voltage to near zero. It also allows the amplifier to use depletion loads for low power operation. The AC output from lead zirconate titanate (PZT) human-body kinetic energy harvesters is expected to range from 100 mV to 5 V. The full-wave active rectifier is designed for fabrication on the PZT harvester and for use with a load resistance as small as 10 k Ω . Fig. 8 shows the schematic of the fabricated rectifying circuit. Measured performance for the first generation circuit demonstrates that rectification was achieved. The maximum power draw was 150 nW, and the output voltage was approximately 90% of the input voltage. This is a key result demonstrating that active rectification is possible using ZnO TFT.

Both kinetic and thermoelectric energy harvesting from the body are gaining traction as solutions for powering wearable, battery-less devices. Future opportunities lie in determining the optimal body location for each particular method of energy harvesting to ensure that the maximum

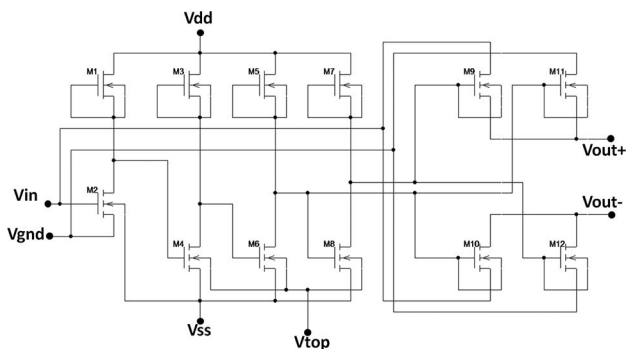


Fig. 8. Circuit layout for ZnO TFT for active electronics on the piezoelectric harvester.

power is harvested. Additionally, there has been limited headway in terms of integrating the rigid energy harvesters into flexible, wearable form factors. Exploring textile material properties to further enable wearable integration for both the kinetic and thermoelectric energy harvesters are also future directions for body harvesting. Finally, ASSIST is also developing energy storage solutions using innovations in supercapacitor electrode design, electrolyte chemistries and membrane fabrication to achieve high-energy density storage capability that exceeds 250 J/cc. These capacitors have been incorporated in ASSIST photo-plethysmogram (PPG) sensor platforms, which are discussed in detail in Section IV-A

III. ULTRA LOW POWER ELECTRONICS

Critical components of any flexible and wearable system are the electronics used for interfacing to sensors, computations for extracting information from data, storage, power harvesting and management, and wireless communication. Most wearable systems now use Commercial off-the-shelf (COTS) components combined onto a printed circuit board (PCB). The major limitation of this approach is that most COTS chips consume too much power to allow for continuous operation from harvested energy without heavy duty cycling. Recent research is moving toward higher degrees of integration with most of the electronics integrated onto a single system on chip (SoC), which helps to reduce size, cost, and power. For example, the SoC in [14] integrates an entire bioelectric wireless sensor onto one chip. The SoC consumes only 19 μ W while measuring electrocardiogram (ECG), extracting heart rate, and sending heart rate information over the radio and can run exclusively off of harvested energy from body heat using a thermoelectric generator (TEG) without any battery at all. These types of SoCs promise to continue the march toward flexible and self-powered wearable sensors.

Two major challenges confronting this vision are power harvesting and wireless communication power. Power

harvesting requires both a harvesting component to convert some ambient energy into an electrical quantity and a harvesting circuit that captures the energy produced by the harvester in a useable form. We discuss TEG harvesters in Section II-A of this paper, but here we consider the challenge of harvesting useable energy from a TEG. The output voltage of the TEG depends on the thermal gradient across the TEG, which as was discussed above, can be quite small ($< 1-2$ °C) for a range of body worn conditions. This results in an output voltage value that can be only a few tens of millivolts. A boost converter is used to convert the low voltage DC output of a TEG into a higher, useable voltage on a storage node like a capacitor. However, the boost converter needs to have power available in order to work, so it cannot operate when there is no power available initially. This creates a Catch 22—one can harvest power, but one also needs power to achieve the harvesting. Hence, there needs to be a mechanism for getting the boost converter started initially. One approach is to power it using a separate mechanism only at startup, and this has been achieved using mechanical or RF methods. Another approach is to construct a circuit that allows the boost converter to start by itself if the input voltage reaches a sufficiently high voltage. This approach is called a cold start. However, for cold start operation, there is a need for a boost converter that can turn on at a few hundred millivolts (so it can begin operation without intervention when the TEG harvesting conditions are good) and continue to harvest energy from the TEG down to very low voltages (so that harvesting can continue even when conditions are poor).

A recent demonstration of a boost converter for TEG harvesting achieved a cold start of 220 mV and a minimum input harvesting voltage below 10 mV [15]. This permits the harvester to continue to power the rest of the circuits

even when the TEG is outputting extremely low voltages due to poor conditions, which can dramatically extend the lifetime of the self-powered system. Further, the efficiency of this boost converter was measured at 53% with a 20 mV input and up to 83% with a 300 mV input, providing more of the available power to the storage node in the system. This type of harvesting circuit will need to be increasingly co-designed with harvesting materials in future self-powered systems.

Wireless communication is the largest power consumer in most body sensor systems. For energy harvesting sensors, the power budget is a system level constraint set by how much power can be reasonably harvested in a small form factor. Since harvesters can only generate a few tens of microwatts per square centimeter, $30 \mu\text{W}$ is a reasonable system level power target. To achieve system power budget targets in the $< 30 \mu\text{W}$ range, the radios in a body sensor system will have to avoid conventional approaches.

Fig. 9 shows the active power consumption of receivers recently reported in literature as a function of their sensitivity (lower sensitivity means farther communication range), grouped by modulation format. The first observation from this plot is that all radios exceed the average power budget ($< 30 \mu\text{W}$) of what's reasonable to harvest from the body today. This requires a receiver solution that significantly improves on the state of the art. We describe one such ultra low-power receiver later in this section. By lowering the power substantially for the receiver, we meet the ASSIST system needs by allowing continuous RF connectivity while operating from harvested energy. Second, there is a significant power penalty for longer-range communication (which is possibly made by lower sensitivity receivers on the left of the plot). Most COTS radios today are designed for the worst-cases: farthest range, most congested wireless environment, highest data rate, etc. This

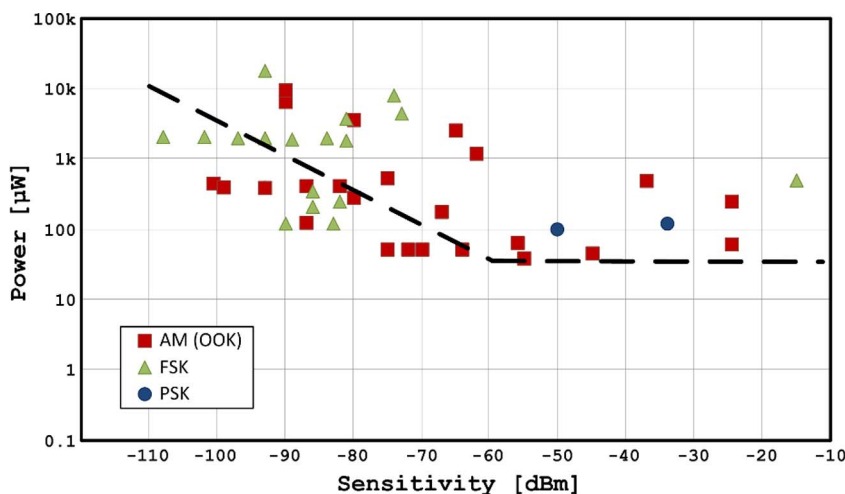


Fig. 9. Plot of receiver power consumption vs. sensitivity (range) for recently reported low-power radios across different modulation schemes (AM (OOK): amplitude modulation (on-off keying); FSK: frequency shift keying; PSK: phase shift keying).

over-margining, combined with the added complexity of supporting many layers of standards, is one factor contributing to the high power consumption of these radios. To meet ASSIST needs, we leverage the fact that the body environment allows for shorter-range communication. The radio we describe below takes advantage of shorter range to reduce sensitivity and then trades this off for significant power savings.

Heavy duty cycling in wireless sensor nodes (WSN) is necessary for ultra-low power consumption, but this results in the node radios spending most of their time in a low power sleep state. A wake-up radio (WRX), being active all the time, is a good solution for wirelessly taking a sensor node out of sleep. The majority of power in WRXs is consumed in the RF front-end in order to improve sensitivity, which is a measure of how small a signal a receiver can sense (analogous to being able to hear better), but high sensitivity is not always required for many applications. Reducing the sensitivity of the radio reduces the radio's power without limiting its functionality in applications like body area networks where communication distance is not much farther than a few meters (around the body).

A 116 nW wake-up radio has recently been demonstrated, complete with crystal reference, interference compensation, and baseband processing, such that a selectable 31-bit code is required to toggle a wake-up signal [16]. The front-end operates over a broad frequency range, tuned by an off-chip band-select filter and matching network. This radio was demonstrated in the 402–405 MHz MICS band and the 915 MHz and 2.4 GHz ISM bands with sensitivities of -45.5 dBm, -43.4 dBm, and -43.2 dBm, respectively. Additionally, the baseband processor implements automatic threshold feedback to detect the presence of interferers and dynamically adjust the receiver's sensitivity. The jamming problem inherent to previous energy-detection wake-up radios is thus mitigated.

There are still challenges in the area of low power electronics that need to be overcome for producing complete self-powered autonomous systems. These include wireless communication at average power levels $< 10 \mu\text{W}$, digital signal processing at $< 3 \mu\text{W}$, extremely low power "always on" blocks like the wakeup radio and clock source, and low leakage. The overall goal would be to get a total electronics power of less than $500 \mu\text{W}$, including all sensors. Researchers in ASSIST are actively working to address these barriers.

IV. FLEXIBLE PHYSIOLOGICAL AND ENVIRONMENTAL SENSORS

The immediately striking limitation in current wearable systems is the human interface. The most common vital signs are temperature, heart rate, respiratory rate, arterial blood pressure, blood oxygen saturation and electrocardiograms where these physiological sensors need to be in contact with the body. These are either worn as an accessory such as a wrist watch, or attached to the skin as an

electronic patch or chest strap hidden under the garment or embedded into the clothing. These sensors are prone to detachment causing performance degradation or interruption by time. The artifacts caused by the user mobility also degrades the signal to noise ratio where simple filtering approaches fall short due to the overlap between the frequency band of the motion and desired signal. However, motion artifacts still can be reduced by statistical or probabilistic approaches or artificial intelligence through multivariate statistical analysis, Kalman filtering and genetic algorithm/neural networks respectively. Below is a description of sensors that have been optimized to consume very low power levels while also providing flexibility and wearability.

A. Photoplethysmogram

As a collaborative technology demonstrator, ASSIST has developed a wireless, wrist-worn platform for continuous monitoring of physiological and environmental parameters during the activities of daily life with the aim of obtaining high statistical correlation between physiological and environmental parameters. The first version of this platform, Soliband (Fig. 10) [17], is solar powered and demonstrates the capability to produce photoplethysmogram (PPG) signals while providing inertial measurement based activity monitoring using COTS integrated circuits. To adhere to a low power budget for solar-powering, a

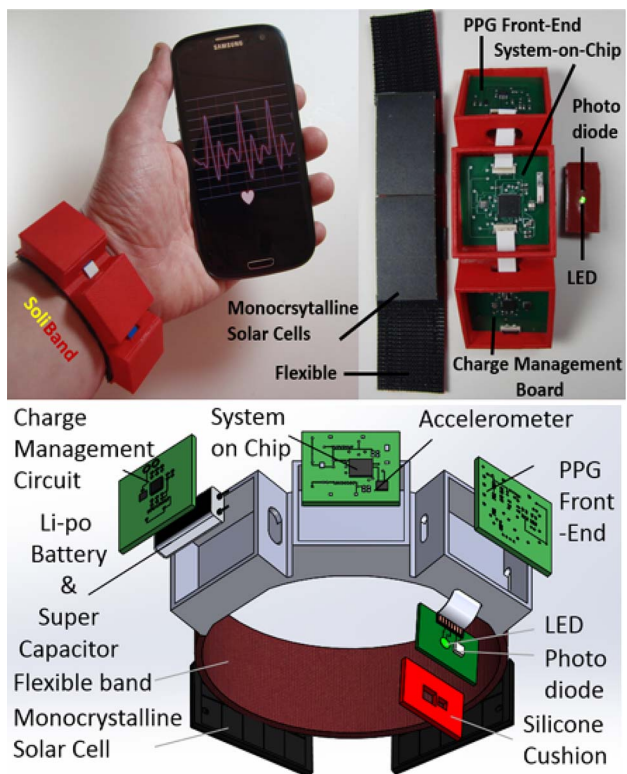


Fig. 10. Soliband wearable wristband.

green light (574 nm) source was used to obtain PPG from the radial artery with minimal signal conditioning. The typical PPG systems use red and near-infrared light to differentiate the concentrations of oxygenated and deoxygenated hemoglobin in the arteries. These wavelengths are highly absorbed in the tissue and limits the performance of reflectance measurements where the light source and the detector are located adjacently and the backscattered photons travelling through the tissue are analyzed. Shorter wavelengths provide a shorter mean free path, causing an increase in backscatter, translating to an increase in the quantity of returned photons, but with a decrease in photon penetration depth. Because of the superficial location of the radial artery, this decrease in penetration depth was irrelevant. The additional benefits of using 574 nm light is the increased absorption coefficient of deoxy- and oxy-hemoglobin over traditional red and infrared wavelengths as well as a decreased absorption coefficient for water. With a higher absorption coefficient, the effect of change in hemoglobin concentration causes an increase in the peak to peak value of measured arterial pulses.

The system incorporated two monocrystalline solar cells to charge-up the onboard 20 mAh lithium polymer battery. Bluetooth Low Energy (BLE) was used to tether the device to a smartphone where a mobile app makes the phone an access point to a dedicated server for long term continuous storage of data. Two power management schemes have been proposed depending on the availability of solar energy. During low light situations, if the battery was low, the device obtained a five-second PPG waveform every minute to consume an average power of 0.57 mW. In situations where the battery was at a sustainable voltage, the device was set to enter its normal 30 Hz acquisition mode, consuming around 13.7 mW.

Reliable solar powering of SoliBand required flexible electrochemical capacitors to maximize the energy density and minimize the charging time while maintaining a low profile device. Initially, a commercially available electrochemical double layer capacitor (EDLC) from Murata was incorporated into the device. This aqueous type EDLC, however, occupies a total volume of 1.14 cm³, imposing limitations on the physical structure of the device. To overcome this, the ASSIST center is developing a high voltage, single cell capacitor to increase the power density per volume through the reduction of equivalent series resistance (ESR) [17]. For this, the electrode resistance for carbon electrodes was reduced by careful design of surface area, porosity and conductivity. For the fabrication of the electrodes, high purity carbon spheres were first synthesized with a low oxygen content (less than 2%). Electrodes were then fabricated by mixing 85%wt carbon, 10%wt Teflon binder and 5%wt acetylene black and punched out to produce an electrode with an area of 0.4 cm² and a thickness of 100 microns. These electrodes were then used to fabricate both Lithium-Ion capacitors and EDLCs [18], [19]. While comparing these fabricated capacitors to a

commercial one is not a straightforward process, a preliminary experiment was performed to show that performance metrics were similar [17]. One important feature to note is that the commercial component consisted of five cells, while the fabricated capacitor was a single cell component. This implies that ASSIST fabricated capacitors have a significantly larger power density per volume.

B. Flexible Electrodes for Wearable Platforms

The ASSIST Center also focuses on the design of flexible, stretchable and durable interconnects for wearable sensing applications ranging from bioelectric sensors to harvesting to storage. Current work in this area has resulted in several key breakthroughs [20]–[24] using screen printing of inks [20] and embroidering of conductive yarns on textile surfaces (see Fig. 11). However, the electrical properties of these interconnects vary under cyclic extensions. To overcome this issue, ASSIST is utilizing inexpensive and highly stretchable and recoverable polymer films along with hot laminations techniques to integrate the printed conductive flexible films onto textiles. This technique enables integrations of microelectronic devices and printed circuit boards on stretchable textiles for wearable monitoring systems or devices (see Fig. 12).

Recently, ASSIST has demonstrated a textile based printed electrodes for biopotential signal monitoring. Wet/gel based electrodes suffer from gel dry-out problems and may not be fully integrated into a wearable platform. However, the printed textile based electrodes conforms to the body surface well, and can be integrated into clothes due to the flexible and breathable nature of textiles. Printed biosignal monitoring electrodes utilizes a screen-printing method, which is a scalable and industry-adopted method to fabricate inexpensive valuable products (see Fig. 13). Utilization of this technique provides cheap and body conformable electrode solutions to be used for potential long-term biopotential monitoring applications (see Fig. 14).

C. Silver Nanowires for Health Sensing

Despite the tremendous progress of nanowire (NW) based flexible electronics, wearable electronics that can deform in response to human motion and be conformal to curvilinear human skin requires a certain level of stretchability [25]. Microfabricated ribbons have led to exciting advances in stretchable electronics, where prestrain-induced buckling of ribbons are responsible for the stretchability [26]. Following the same strategy, Si NWs have been explored for stretchable electronics [27], [28]. Si NWs were transferred to a prestrained Polydimethylsiloxane (PDMS) substrate. Upon release of the substrate, the Si NWs buckled into not only the common wavy shape of micro-ribbons, but also the 3D coiled shape. The buckling shape was controlled by surface treatment of the PDMS substrate [28]. The 3D coiled shape is more stretchable than the wavy shape. Challenges for NW-based stretchable

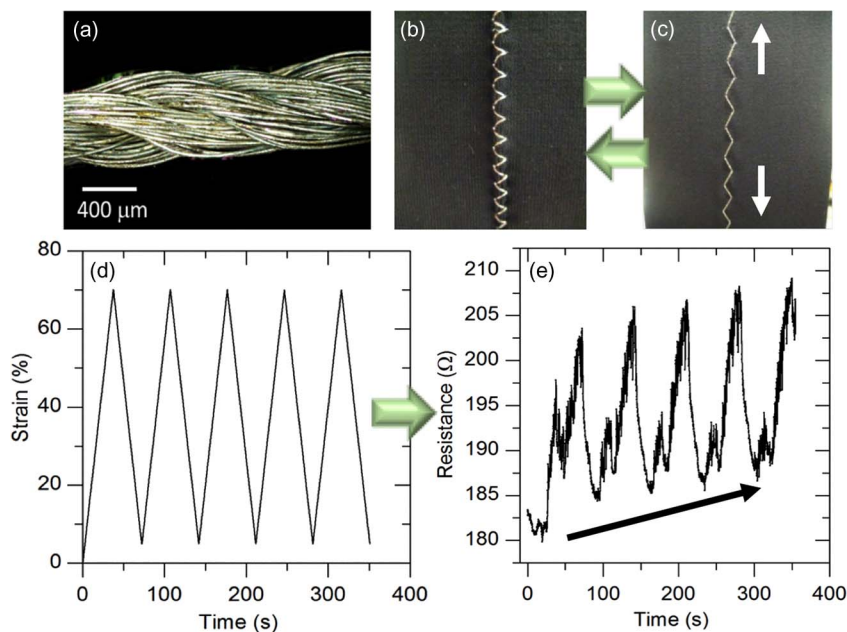


Fig. 11. (a) Ag-plated yarns are stitched into compression fabrics in a (b)–(c) zig-zag pattern so as to assist in controlling the resistance changes with stretching. (d) Oscillation of the 70% strain/stretching results (e) < 10% changes in the resistance with a nonstretched baseline drift to an increasing resistance. While the current path is not changed upon stretching, localized deformation of the yarn’s twist construction can result in changes in the filament-to-filament percolation network for electrical conduction.

electronics like transistors include NW assembly (alignment) on stretchable substrates, high-quality, stretchable gates, and reliable contacts under stretching. Recently, NW-based stretchable conductors and related sensors have attracted much attention for wearable electronics and sensors [29], [30]. As an example, AgNW conductors have been fabricated by embedding AgNW network below the surface of elastomeric PDMS substrate. The AgNWs can be printed into different shapes and patterns. The AgNW/PDMS composite is highly conductive (conductivity > 5000 S/cm) and has a higher stretchability (> 50% strain with constant conductivity). In addition, the AgNW network is below the PDMS surface, thus making

the conductor mechanically robust under thousands of cycles without delamination and cracking [29]. Fig. 15 shows the electric performance of the AgNW conductors as a function of strain and the underlying mechanism for the high stretchability. These highly stretchable conductors can be used as conformal, wearable electrodes for bioelectronic sensing. In the case of ECG electrodes, AgNW dry electrodes have outperformed the conventional wet Ag/AgCl electrodes with less motion artifacts. It should be emphasized here that these AgNW electrodes do not use the electrolytic gel layer, which make them suitable for long-term wearing. Sandwiching a dielectric layer with two such conductors can form a capacitive sensor.

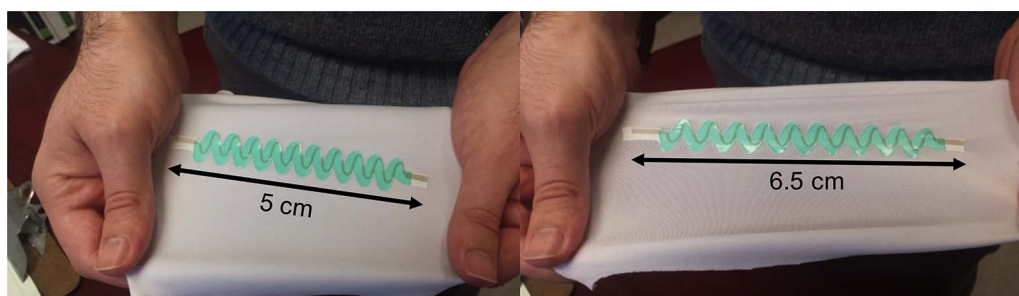


Fig. 12. Example of an “iron on” fabrication of a flexible sinusoidal interconnect on a knitted compression fabric. Prior to stretching (left) the resistance of the 1 mm line printed on a thermoset polyurethane is 42 Ohms. A 30% strain increases the resistance by 165% (right). A more moderate 4% strain results in < 2% change in resistance and a < 4% baseline drift over 50 stain oscillations. Increased strain and strain cycling induces crack formation within the printed ink, which consists of a metallic flake and polymer binder complex.

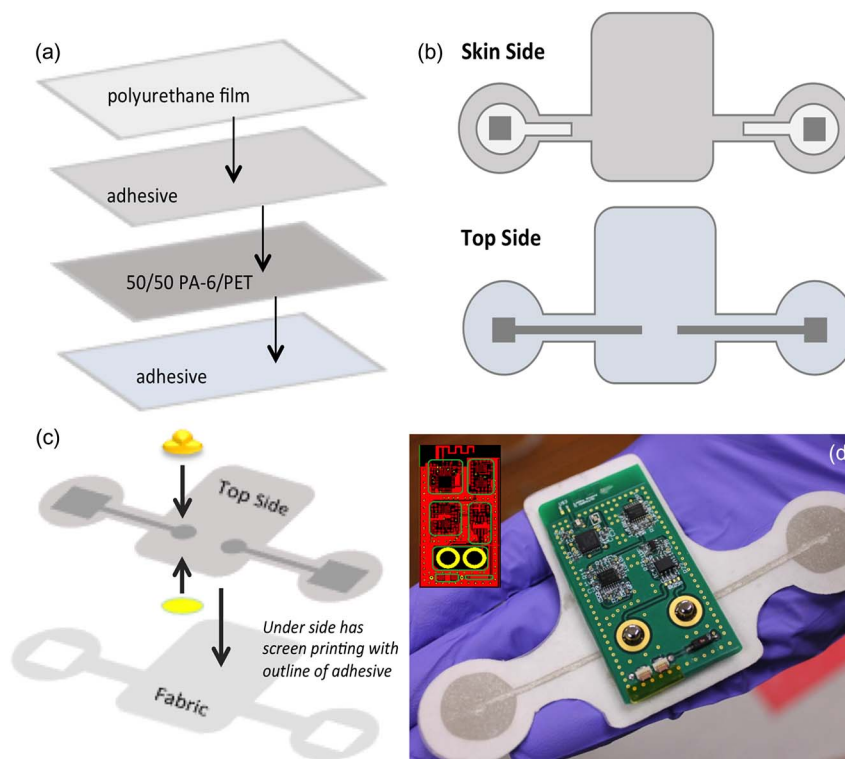


Fig. 13. Custom biopotential measurement patches are fabricated using an (a) multilayered structure of polyurethane films and a 50/50 PET/PA6 bicomponent nonwoven. (b) Each layer is die cut to expose Ag/AgCl electrodes to the skin, surrounded by adhesive and a flexible Ag interconnect leading to (c) interconnect snaps. The female end of the snap is built into the (d) PCB board circuitry for modular, reusable placement.

Following this principle multifunctional wearable sensors have been developed. Such sensors can detect strain (up to 50%), pressure (up to ~ 1.2 MPa) and finger touch with high sensitivity, fast response time (~ 40 ms) and good pressure mapping function [32]. ASSIST sensors have been demonstrated for several wearable applications including monitoring thumb movement, sensing the strain of the knee joint in patellar reflex (knee-jerk) and other human motions such as walking, running and jumping from squatting, thus illustrating the potential utility of such sensors in robotic systems, prosthetics, healthcare and flexible touch panels. Fig. 15(b) and (c) show a pressure sensor array and an ECG electrode, respectively.

D. Metal–Oxide Nanowires for Gas Sensing

Since a key aspect of the Center’s research is correlating health and environment, a key element of ASSIST sensor technology is the correlation of toxic gases, such as ozone, in the environment with associated health responses such as wheezing and EKG. According to the National Ambient Air Quality Standards (NAAQS), the maximum 8-hour average ozone concentration is 75 parts-per-billion (ppb) and 1-hour average ozone concentration is 120 ppb while the background ozone in the United States is between 18 to 36 ppb [33]. Hence, any sensor used for such applications must have the right sensitivity to meet the guidelines

above. In addition, they must also have the appropriate selectivity against other gases, low total power consumption, stability, accuracy, reliability, and low cost. The right combination of the requirements depend on the application, for example, high parts-per-million (ppm) levels are sufficient for industrial detection, whereas ppb levels are needed for more precise monitoring.

While several solutions are available for gas sensing, solid-state-based thin film sensors are preferred for real-time and long-term environmental monitoring [34]–[37]. Metal–oxide-based thin-film sensors are widely used but typically require high temperatures (> 300 °C) operation to heat the substrate [34]. This comes at the cost of large power consumption (in the mW range) that is not desirable in a wearable platform. In addition, specificity and drift are also challenges facing metal–oxide gas sensors. Recent efforts to overcome these barriers include the use of nanowires [35], [36], self-heated nanowires [37] and use of AlGaN/GaN structures [38]. ASSIST’s approach towards addressing the key barriers in gas sensing are focused on atomic layer deposited (ALD) ultra thin metal oxide layers that exhibit sensitivity to ozone sensitivity down to 20 ppb. ALD is a widely known technique for depositing ultrathin films with precise control of thickness and composition as well as for conformal coatings of high surface areas.

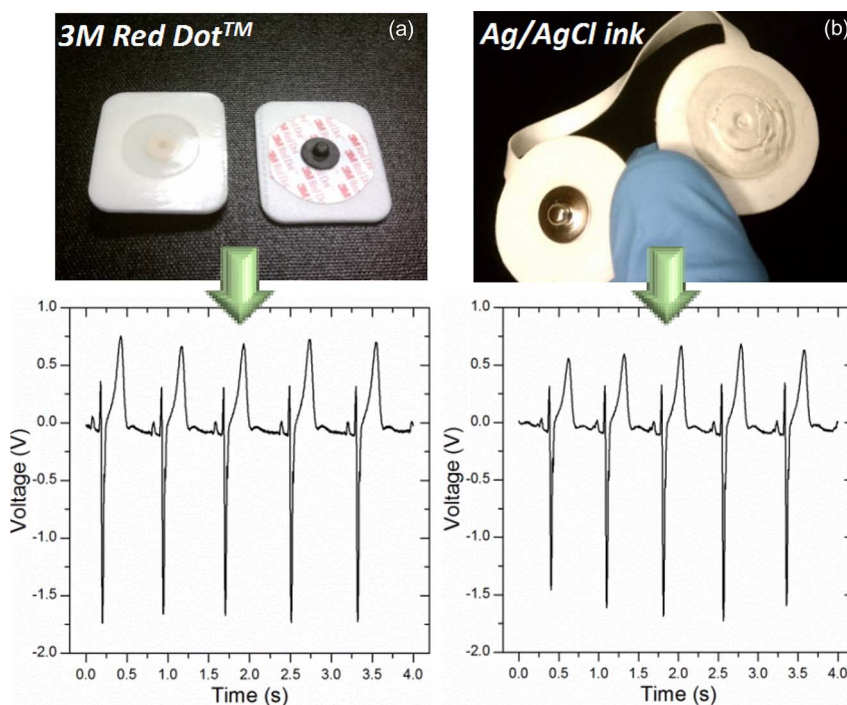


Fig. 14. ECG signal comparison between (a) 3M Red Dot wet electrodes and (b) custom nonwoven supported screen print Ag/AgCl dry electrode developed in the ASSIST Center. Comparison is made with similar surface at a frequency of 120 Hz General Electric bedside monitor (GE Dash 4000, WI USA). This Ag/AgCl ink, obtained from Creative Materials (124-36) was used for the modular/reusable patch shown in Fig. 13(d).

Fig. 16 shows the response of an ALD deposited 6 nm SnO₂ gas sensor operated at room temperature to ozone. It was observed that the ALD SnO₂ gas sensor achieves ozone sensitivity in the 50–100 ppb range [see Fig. 16(b)]. It is believed that the precise control of metal oxide thickness

afforded by the ALD is directly related to the excellent sensitivity of the sensors observed at room temperature. This thickness dependence can be understood as follows: it is well known that the electron trapping associated with the adsorbed gas molecules induces band bending and

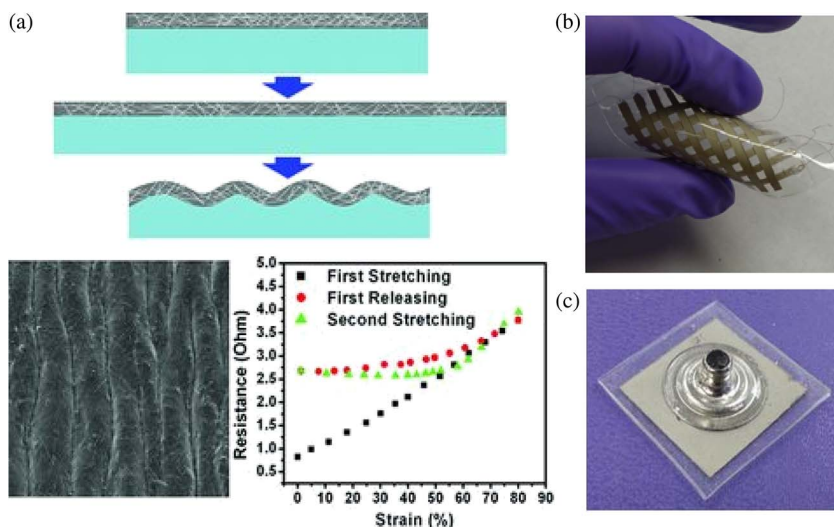


Fig. 15. (a) Highly conductive and stretchable AgNW conductor, (top) schematic to show the formation of stretchable (wavy) surface that is key to the high stretchability, (bottom left) SEM image of the wavy surface, (bottom right) electric performance as a function of strain. (b) Pressure sensor array based on capacitors made of the AgNW conductors. (c) ECG electrode made of AgNW conductor.

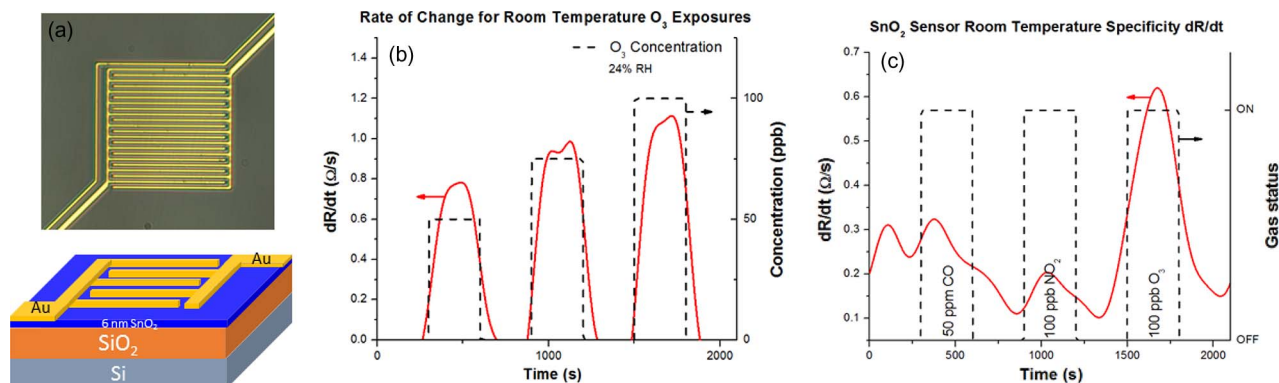


Fig. 16. (a) Optical image (above) and schematic diagram (below) of the fabricated SnO₂ gas sensor (b) Room temperature transient response of the ALD SnO₂ thin film sensor for 50 ppb, 75 ppb, and 100 ppb of ozone (O₃) exposure and (c) Room Temperature transient responses of the ALD SnO₂ thin film sensor for 50 ppm CO, 100 ppb NO₂, and 100 ppb O₃ exposure. Relative large response to ozone was obtained by ALD SnO₂ thin film sensor.

electron depletion region in the metal oxide which is typically indicated by the Debye length. This change in band bending relative to the different gas concentrations results in a change of the resistance of the metal oxide when measured between two electrodes [see Fig. 16(a)]. The magnitude of change of the metal-oxide resistance will depend critically on the relationship of the Debye length and the bulk metal oxide thickness. Hence controlling the thickness will have a large impact on sensitivity. This large sensitivity in turn mitigates the need for heating the sensor, which in turn results in very low power consumption. Specificity measurements were also conducted by measuring the sensor response in CO and NO₂. As shown in Fig. 16(c) the SnO₂ sensor shows a much larger response to ozone compared to CO or NO₂. With the large sensitivity with the room temperature operation that reduces the total power consumption to μ W range and intrinsic sensitivity against NO₂ and CO, it is evident that ALD based metal oxide sensors are promising for long term measurements of environmental gases in a wearable platform.

Future ASSIST work in the gas sensing area includes incorporating AlGaN/GaN based structures and assembling multiple metal oxide nanowires heterogeneously on CMOS chips to provide both high sensitivity and high selectivity for not only gases such as ozone but also NO₂, CO and volatile organic compounds (VOCs). ASSIST's recent work on VOCs is discussed in the next section.

E. Capacitive Micromachined Ultrasonic Transducers for Volatile Organic Compound Sensing

As mentioned above, the ASSIST Center is developing low-power, miniaturized, wearable sensors to monitor environmental pollutants continuously and correlate the findings with physiological measurements. For many environmental pollutants high-ppb-to-ppm-level detection is adequate and hence sensitivity can be traded off for power in environmental monitoring applications. In this regard,

in addition to gases such as ozone and NO₂, we are also developing technologies that can provide real-time monitoring of volatile organic compounds (VOCs) using a low-power gas sensor design based on a capacitive micromachined ultrasonic transducer (CMUT), for use on self-powered wearable platforms. The working mechanism of our CMUT resonant sensor is based on mass loading. The CMUT sensor presented here is functionalized with polyisobutylene (PIB), which is sensitive to specific VOCs such as toluene. When the functionalized device is exposed to a VOC, the additional mass of the adsorbed analyte on the resonant structure causes a shift in the resonant frequency. A free-running oscillator designed using the CMUT as the frequency selective device tracks this change in the resonant frequency. Earlier demonstrations of a CMUT-based sensor have shown functionality with 70-mW power consumption operating at 48 MHz, and achieved 51-ppt (parts-per-trillion) resolution for dimethyl methylphosphonate (DMMP), a common simulant of sarin gas in air [39]. In the present work we show a sensor operating at 4.5 MHz and consuming 0.77 mW for environmental monitoring. The sensor comprises a polymer-functionalized CMUT resonator in the feedback loop of a Colpitts oscillator. We fabricated the CMUT resonators using a novel process based on anodic bonding. The cavities and bottom electrodes are formed on a borosilicate glass wafer [see Fig. 17(a) and (b)] [40]. The device layer of an SOI wafer bonded on glass forms the vibrating plate on top of vacuum-sealed cavities. This fabrication approach reduces process complexity and helps minimize parasitic components. CMUTs with center frequencies in the 3–50 MHz range with Q-factors as high as \sim 400 have successfully been fabricated using this process. We used a 4.52-MHz device ($Q = 180$) coated with a thin layer of polyisobutylene (PIB) for sensing of toluene [see Fig. 17(c)]. The sensitivity of the described sensor for toluene is measured as 270 Hz/ppm in the 10–20-ppm concentration range. The electrical oscillator exhibits a

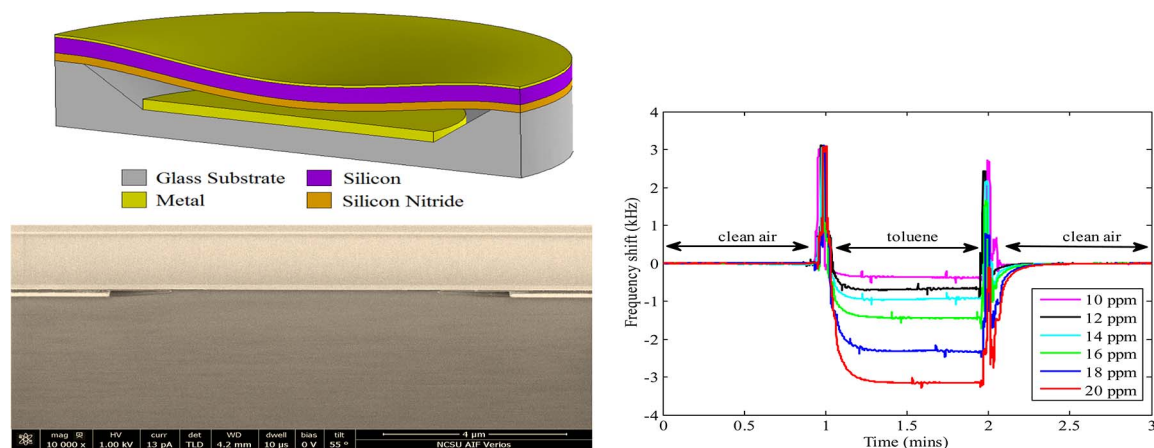


Fig. 17. (a) The schematic cross-section of a CMUT cell showing different layers in the transducer structure. (b) The scanning electron microscope (SEM) image of the CMUT cross-section. (c) Sensor output for different concentrations of toluene in the 10-20-ppm range. Clean air was first flowed for 1 min, followed by toluene for 1 min, and clean air again for 1 min.

minimum Allan deviation of 3.15 Hz (3σ), which is a measure of the short-term frequency stability. Accordingly, the resolution of the sensor is calculated as 12 ppb (3σ). Considering that the OSHA permissible exposure limit for toluene is 200 ppm (time weighted average) [41], the presented sensor is clearly capable of monitoring toluene with high resolution and sensitivity. Our current efforts focus on further quantification of sensor performance and extension of the demonstrated sensor platform to multiple channels for improved selectivity to detect a variety of VOCs.

V. CONCLUSION

The ASSIST Center has developed several flexible, ultra-low-power, multimodal technologies that enable wearable systems to be effective in longitudinal health and wellness monitoring, with a particular emphasis on enhancing their comfort, lifetime, and functionality to improve user compliance and extend the potential applications and user groups of such systems. These technologies include:

- high-efficiency nanostructured energy harvesters for body heat and body motion harvesting and high energy density storage capacitors;
- low power computation and communication strategies to significantly lower power consumption via ultra low voltage boost converters and a 115 nW wake up radio;
- new sensing modalities for physiological and environmental sensing that consume less power while monitoring EKG, PPG, hydration, pressure, environmental gas and VOC sensing;

- novel flexible materials that provide form, function and comfort, all hierarchically integrated through scales ranging from enabling nanoscale materials and devices to the human body interface.

As a demonstration platform, we have developed a solar-powered, wireless, wrist-worn platform for continuous monitoring of physiological and environmental parameters during the activities of daily life. In this platform, the capability to produce photoplethysmogram (PPG) and actigraphy signals was demonstrated, which was enabled by careful analysis of photon-tissue interaction, design of power management and improvement in the charge storage capacity of our custom super-capacitors.

Advances in these technologies present a unique opportunity for achieving a high-performance, multifunctional, self-powered sensing system. These systems enable correlation of personal environmental exposure to health response, including impacts on chronic conditions (e.g., asthma, heart disease, etc.), providing an enhanced understanding of onset and progression of disease and its effective management. ■

Acknowledgment

The authors would like to acknowledge the students and scientists who contributed to this work: Francisco Suarez, Charles Yeager, Michael Lim, Steven Mills, Murat Yokus, Ryan Hodges, Rachel Foote, James Dieffenderfer, Amanda Myers, Shanshan Yao, J. Israel Ramirez, Haoyu Li, Eric Beppler, Brinnae Bent, Marzana M. Mahmud, Juan Li, Jean E. Lunsford, Xiao Zhang, Dr. Ramakrishnan Rajagopalan, Dr. Clive Randall, Dr. F. Yalcin Yamaner, and Dr. H. Troy Nagle.

REFERENCES

- [1] D. Ledger and D. McCaffrey, *Inside Wearables*, 2014. [Online]. Available: <http://endeavour-partners.net/assets/Endeavour-Partners-Wearables-and-the-Science-of-Human-Behavior-Change-Part-1-January-20141.pdf>
- [2] W. Glatz, E. Schwyter, L. Durrer, and C. Hierold, "Bi₂Te₃-based flexible micro thermoelectric generator with optimized design," *J. Microelectromech. Syst.*, vol. 18, no. 3, pp. 763–772, 2009.
- [3] S. Kim, J. We, and B. Cho, "A wearable thermoelectric generator fabricated on a

- glass fabric," *Energy Environ. Sci.*, vol. 7, no. 6, pp. 1959–1965, 2014.
- [4] N. Satyala, P. Norouzzadeh, D. Vashae, and N. Bulk, "Thermoelectrics: Concepts, Techniques, Modeling, Book chapter," in *Thermoelectrics at Nanoscale*. New York, NY, USA: Springer, 2014, pp. 141–183.
- [5] K. A. Cook-Chennault, N. Thambi, and A. M. Sastry, "Powering MEMS portable devices—a review of non-regenerative and regenerative power supply systems with special emphasis on piezoelectric energy harvesting systems," *Smart Mater. Struct.*, vol. 17, no. 4, p. 043001, 2008.
- [6] S. Priya, "Advances in energy harvesting using low profile piezoelectric transducers," *J. Electroceram.*, vol. 19, no. 1, pp. 167–184, 2007.
- [7] P. L. Green, E. Papatheou, and N. D. Sims, "Energy harvesting from human motion and bridge vibrations: An evaluation of current nonlinear energy harvesting solutions," *J. Intell. Mater. Syst. Struct.*, vol. 24, no. 12, pp. 1494–1505, 2013.
- [8] M. A. Karami and D. J. Inman, "Powering pacemakers from heartbeat vibrations using linear and nonlinear energy harvesters," *Appl. Phys. Lett.*, vol. 100, no. 4, p. 042901, 2012.
- [9] P. Pillatsch, E. M. Yeatman, and A. S. Holmes, "A piezoelectric frequency up-converting energy harvester with rotating proof mass for human body applications," *Sens. Actuators, A: Phys.*, vol. 206, pp. 178–185, 2014.
- [10] C. B. Yeager, Y. Ehara, N. Oshima, H. Funakubo, and S. Trolrier-McKinstry, "Dependence of e_{31} , f on polar axis texture for tetragonal $\text{Pb}(\text{Zr}_x, \text{Ti}_{1-x})\text{O}_3$ thin films," *J. Appl. Phys.*, vol. 116, no. 10, p. 104907, 2014.
- [11] C. B. Yeager and S. Trolrier-McKinstry, "Epitaxial $\text{Pb}(\text{Zr}_x, \text{Ti}_{1-x})\text{O}_3$ ($0.30 \leq x \leq 0.63$) films on (100)MgO substrates for energy harvesting applications," *J. Appl. Phys.*, vol. 112, no. 7, p. 074107, 2012.
- [12] H. Yeo and S. Trolrier-McKinstry, "001 oriented piezoelectric films prepared by chemical solution deposition on Ni foils," *J. Appl. Phys.*, vol. 114, no. 1, p. 014105, 2014.
- [13] Y. Li, J. Ramirez, K. Sun, and T. N. Jackson, "Low-voltage double-gate ZnO thin-film transistor circuits," *IEEE Electron Device Lett.*, vol. 34, no. 7, pp. 891–893, 2013.
- [14] Y. Zhang et al., "A batteryless 19 μW MICS/ISM-band energy harvesting body sensor node SoC for ExG applications," *IEEE J. Solid State Circuits*, vol. 48, no. 1, pp. 199–213, 2013.
- [15] A. Shrivastava, D. Wentzloff, and B. H. Calhoun, "A 10 mV-input boost converter with inductor peak current control and zero detection for thermoelectric energy harvesting," in *Proc. IEEE Custom Integr. Circuits Conf. (CICC)*, San Jose, CA, USA, 2014.
- [16] S. Oh, N. E. Roberts, and D. D. Wentzloff, "A 116 nW multi-band wake-up receiver with 31-bit correlator and interference rejection," in *Proc. IEEE Custom Integr. Circuits Conf. (CICC)*, San Jose, CA, USA, 2013.
- [17] J. Dieffenderfer et al., "Solar powered wrist worn acquisition system for continuous photoplethysmogram monitoring," in *Proc. 36th Int. Conf. IEEE Eng. Med. Biol. Soc. (EMBC'14)*, Chicago, IL, 2014.
- [18] J. Kalupson, D. Ma, C. A. Randall, R. Rajagopalan, and K. Adu, "Ultrahigh-power flexible electrochemical capacitors using binder-free single-walled carbon nanotube electrodes and hydrogel membranes," *J. Phys. Chem. C.*, vol. 118, no. 6, pp. 2943–2952, 2014.
- [19] W. Qu, E. Dorjpalam, R. Rajagopalan, and C. A. Randall, "Role of additives in formation of solid-electrolyte interfaces on carbon electrodes and their effect on high-voltage stability," *Chem. Sus. Chem.*, vol. 7, no. 4, pp. 1162–1169, 2014.
- [20] Z. Fan et al., "Toward the development of printable nanowire electronics and sensors," *Adv. Mater.*, vol. 21, no. 37, pp. 3730–3743, 2009.
- [21] S. Ju et al., "Fabrication of fully transparent nanowire transistors for transparent and flexible electronics," *Nature Nanotechnol.*, vol. 2, no. 6, pp. 378–384, 2007.
- [22] X. Duan et al., "High-performance thin-film transistors using semiconductor nanowires and nanoribbons," *Nature*, vol. 425, no. 6955, pp. 274–278, 2003.
- [23] M. McAlpine, H. Ahmad, D. Wang, and J. Heath, "Highly ordered nanowire arrays on plastic substrates for ultrasensitive flexible chemical sensors," *Nature Mater.*, vol. 6, no. 5, pp. 379–384, 2007.
- [24] K. Takei et al., "Nanowire active-matrix circuitry for low-voltage macroscale artificial skin," *Nature Mater.*, vol. 9, no. 10, pp. 821–826, 2010.
- [25] J. A. Rogers, T. Someya, and Y. Huang, "Materials and mechanics for stretchable electronics," *Science*, vol. 327, no. 5973, pp. 1603–1607, 2010.
- [26] D. Khang, H. Jiang, Y. Huang, and J. A. Rogers, "A stretchable form of single-crystal silicon for high-performance electronics on rubber substrates," *Science*, vol. 311, no. 5758, pp. 208–212, 2006.
- [27] S. Ryu et al., "Lateral buckling mechanics in silicon nanowires on elastomeric substrates," *Nano Lett.*, vol. 9, no. 9, pp. 3214–3219, 2009.
- [28] F. Xu, W. Lu, and Y. Zhu, "Controlled 3D buckling of silicon nanowires for stretchable electronics," *ACS Nano*, vol. 5, no. 1, pp. 672–678, 2011.
- [29] F. Xu and Y. Zhu, "Highly conductive and stretchable silver nanowire conductors," *Adv. Mater.*, vol. 24, no. 37, pp. 5117–5122, 2012.
- [30] P. Lee et al., "Highly stretchable and highly conductive metal electrode by very long metal nanowire percolation network," *Adv. Mater.*, vol. 24, no. 25, pp. 3326–3332, 2012.
- [31] W. Hu et al., "Intrinsically stretchable transparent electrodes based on silver-nanowire-crosslinked-polyacrylate composites," *Nanotechnology*, vol. 23, no. 34, p. 344002, 2012.
- [32] S. Yao and Y. Zhu, "Wearable multifunctional sensors using printed stretchable conductors made of silver nanowires," *Nanoscale*, vol. 6, no. 4, pp. 2345–2352, 2014.
- [33] U.S. Environmental Protection Agency, Technology Transfer Network, National Ambient Air Quality Standards (NAAQS). [Online]. Available: <http://www.epa.gov/ttn/naaqs/>
- [34] C. Wang, L. Yin, L. Zhang, D. Xiang, and R. Gao, "Metal oxide gas sensors: Sensitivity and influencing factors," *Sensors*, vol. 10, no. 3, pp. 2088–2106, 2010.
- [35] R. Bajpai, A. Motayed, A. V. Davydov, K. A. Bertness, and M. E. Zaghoul, "UV-Assisted Alcohol sensing with Zinc oxide functionalized Gallium Nitride Nanowires," *IEEE Electron Device Lett.*, vol. 33, no. 7, pp. 1075–1077, 2012.
- [36] S. P. Arnold, S. M. Prokes, F. K. Perkins, and M. E. Zaghoul, "Design and performance of a simple, room-temperature Ga_2O_3 nanowire gas sensor," *Appl. Phys. Lett.*, vol. 95, no. 10, p. 103102, 2009.
- [37] J. D. Prades et al., "Ultralow power consumption gas sensors based on self-heated individual nanowires," *Appl. Phys. Lett.*, vol. 93, no. 12, p. 123110, 2008.
- [38] P. Offermans, R. Vitushinsky, M. Crego-Calama, and S. H. Brongersma, "Gas Sensing with AlGaIn/GaN 2DEG Channels," *Procedia Eng.*, vol. 25, pp. 1417–1420, 2011.
- [39] H. J. Lee, K. K. Park, M. Kupnik, Ö. Oralkan, and B. T. Khuri-Yakub, "Chemical vapor detection using a capacitive micromachined ultrasonic transducer," *Anal. Chem.*, vol. 83, no. 24, pp. 9314–9320, Dec. 15, 2011.
- [40] M. M. Mahmud et al., "A low-power gas sensor for environmental monitoring using a capacitive micromachined ultrasonic transducer," in *Proc. IEEE Sensors Conf.*, 2014, pp. 677–680.
- [41] United States Department Occupational Safety and Health Administration, Safety and Health Topics, Toluene, Occupational Exposure Limits. [Online]. Available: https://www.osha.gov/SLTC/toluene/exposure_limits.html

ABOUT THE AUTHORS

Veena Misra (Fellow, IEEE) received the B.S., M.S., and Ph.D. degrees from North Carolina State University (NCSU), Raleigh, NC, USA, in 1990, 1992, and 1995, respectively, all in electrical engineering.

She is a Professor of Electrical and Computer Engineering and the Director of the NSF ERC ASSIST Center at NCSU. Her current research interests include low-power sensors, energy harvesting, and power devices.

Dr. Misra was the recipient of the 2001 NSF Presidential Early Career Award, the 2007 Outstanding Alumni Research Award, and the 2011 Alcoa Distinguished Engineering Research Award.



Jesse S. Jur received the B.S. degree in chemical engineering from The University of South Carolina, Columbia, SC, USA, in 2001, the M.S. degree in chemical and biomedical engineering from Johns Hopkins University, Baltimore, MD, USA, in 2004, and the Ph.D. degree in Materials Science and Engineering from North Carolina State University, Raleigh, NC, USA, in 2007.

From 2009 to 2010, he was a research assistant professor of Chemical and Biomolecular Engineering at North Carolina State University. He is currently an assistant professor of Textile Engineering, Chemistry & Science at North Carolina State University. His current research interests are focused on integrating new nanotechnology methods for supporting electronic materials and devices in wearable fabrics.



Alper Bozkurt received the Ph.D. degree from Cornell University, Ithaca, NY, USA, and the Master's degree in biomedical engineering from Drexel University, Philadelphia, PA, USA.

He is currently an Assistant Professor in Department of Electrical and Computer Engineering at North Carolina State University (NCSU), Raleigh, NC, USA. He is the founder and the director of Integrated Bionic MicroSystems Laboratory at NCSU, where his current research interests include development of microscale sensors, actuators, and methodologies to unlock the mysteries of biological systems with an aim of engineering these systems directly or developing new engineering approaches by learning from them.

Dr. Bozkurt is a recipient of the Calhoun Fellowship from Drexel University, the Donald Kerr Award at Cornell University, the Chancellor's Innovation Award, the William F. Lane Outstanding Teacher Award at North Carolina State University, and the best paper award from The U.S. Government Microcircuit Applications and Critical Technology Conference.



John Lach (Senior Member, IEEE) received the B.S. degree in science, technology, and society from Stanford University, Stanford, CA, USA, in 1996 and the M.S. and Ph.D. degrees in electrical engineering from the University of California, Los Angeles, CA, USA, in 1998 and 2000, respectively.

He joined the faculty at the University of Virginia (UVA) in 2000, where he is currently Professor and Chair of Electrical and Computer Engineering. He is a Co-Founder and Steering Committee member for the *Wireless Health* conference series, a Co-Founder and Co-Director of the UVA Center for Wireless Health, and part of the leadership team for the NSF Nanosystems Engineering Research Center for Advanced Self-Powered Systems of Integrated Sensors and Technologies (ASSIST). His primary research interests include body sensor networks, wireless health, embedded systems, and digital system design methodologies. He has published over 130 refereed papers.

Dr. Lach is a former Associate Editor for the IEEE TRANSACTIONS ON COMPUTERS and the IEEE TRANSACTIONS ON COMPUTER-AIDED DESIGN AND INTEGRATED CIRCUITS AND SYSTEMS, and received five best paper awards.



Benton Calhoun received the B.S. degree in electrical engineering from the University of Virginia, Charlottesville, VA, USA, in 2000, and the M.S. and Ph.D. degrees in electrical engineering from the Massachusetts Institute of Technology, Cambridge, MA, USA, in 2002 and 2006, respectively.

In January 2006, he joined the faculty at the University of Virginia, Charlottesville, VA, USA, in the Electrical and Computer Engineering Department, where he is now the Commonwealth Associate Professor of Electrical and Computer Engineering. He is also co-founder and CTO of PsiKick, Inc. His research interests include self-powered body sensor node (BSN) design, low-power digital circuit design, sub-threshold digital circuits, SRAM design for end-of-the-roadmap silicon, variation tolerant circuit design methodologies, and low-energy electronics for medical applications.



Bongmook Lee received the B.S. degree in electronic materials engineering from the Gwangju University, Seoul, South Korea, in 2002, and the M.S. and Ph.D. degrees in electrical and computer engineering from North Carolina State University, Raleigh, NC, USA, in 2005 and 2010, respectively.

He was a postdoctoral research associate in the NSF Future Renewable Electric Energy Delivery and Management System Center (FREEDM) from 2010 to 2012. He is currently a research assistant professor of Electrical and Computer Engineering and NSF ASSIST center. His current research includes device design, processing, and characterization of the ultra-low-power environmental sensors, high-speed CMOS devices, nonvolatile devices, and wideband gap GaN, and SiC-based power devices.

Dr. Lee was a recipient of student fellowship from Applied Materials, Inc., from 2007 to 2009.



Thomas Jackson, photograph and biography not available at the time of publication.

John Muth, photograph and biography not available at the time of publication.

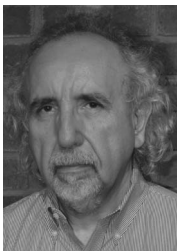
Ömer Oralkan (Senior Member, IEEE) received the B.S. degree from Bilkent University, Ankara, Turkey, in 1995, the M.S. degree from Clemson University, Clemson, SC, USA, in 1997, and the Ph. D. degree from Stanford University, Stanford, CA, USA, in 2004, all in electrical engineering.



He was a Research Associate (2004-2007) and then a Senior Research Associate (2007-2011) in the E. L. Ginzton Laboratory at Stanford University. In 2012, he joined the Department of Electrical and Computer Engineering, North Carolina State University, Raleigh, NC, USA, as an Associate Professor. His current research focuses on developing devices and systems for ultrasound imaging, photoacoustic imaging, image-guided therapy, biological and chemical sensing, and ultrasound neural stimulation. He has authored more than 140 scientific publications.

Dr. Oralkan is an Associate Editor for the IEEE TRANSACTIONS ON ULTRASONICS, FERROELECTRICS, AND FREQUENCY CONTROL and serves on the Technical Program Committee of the IEEE Ultrasonics Symposium. He received the 2013 DARPA Young Faculty Award and the 2002 Outstanding Paper Award of the IEEE Ultrasonics, Ferroelectrics, and Frequency Control Society.

Mehmet Öztürk (Fellow, IEEE) received the B.S. degree in electrical engineering from Boğaziçi University, Istanbul, Turkey, in 1980, and the M.S. degree in electrical engineering from Michigan Technological University, Houghton, MI, USA, in 1983. He continued his graduate studies at North Carolina State University, Raleigh, NC, USA, under Jimmie J. Wortman receiving the Ph.D. degree in electrical and computer engineering in 1988.



After graduation, he joined his department, where he is currently serving as a professor of Electrical and Computer Engineering, where his research focused on novel processes for advanced CMOS ICs with emphasis on applications of Group IV epitaxy in channel and source/drain engineering. His current research interests centers around flexible electronics for energy harvesting, particularly flexible thermoelectric devices for body energy harvesting.

Susan Trolier-McKinstry (Fellow, IEEE) is a Professor of Ceramic Science and Engineering, Professor of Electrical Engineering, Director of the W. M. Keck Smart Materials Integration Laboratory, and Director of the Nanofabrication facility at the Pennsylvania State University, State College, PA, USA. Her main research interests include thin films for dielectric and piezoelectric applications. She is a fellow of the American Ceramic Society and the Materials Research Society, and an academician of the World Academy of Ceramics. She currently serves as an Associate Editor for *Applied Physics Letters*, the *Journal of the American Ceramic Society*, and the IEEE TRANSACTIONS ON ULTRASONICS, FERROELECTRICS, AND FREQUENCY CONTROL. Twenty people that she has advised/co-advised have gone on to take faculty positions around the world.



Daryoosh Vashaee received the Ph.D. degree from the University of California at Santa Cruz, USA.



He worked at the Massachusetts Institute of Technology (MIT), Cambridge, MA, USA, as a postdoctoral scholar, at Oklahoma State University, Stillwater, OK, USA, as an assistant professor, and joined North Carolina State University, Raleigh, NC, USA, in the electrical and computer engineering department as an associate professor in 2014. He is an expert in theoretical and experimental aspects of superlattices and nanostructured materials for energy conversion and sensing applications. In the past, he has contributed to the development of several key thermoelectric structures including heterostructure thermionic devices and bulk nanocomposite materials. His research at ASSIST is focused on development of nanocomposite thermoelectric materials for body heat energy harvesting.

David Wentzloff, photograph and biography not available at the time of publication.

Yong Zhu received the B.S. degree in mechanical engineering from the University of Science and Technology of China, Hefei, China, in 1999, and the M.S. and Ph.D. degrees in mechanical engineering from Northwestern University, Evanston, IL, USA, in 2001 and 2005, respectively.



Since 2007, he has been with North Carolina State University, Raleigh, NC, USA, where he is currently an Associate Professor in the Department of Mechanical and Aerospace Engineering. His group conducts basic and applied research at the intersection of solid mechanics and micro/nano-technology, including nanomechanics, micro/nano-electromechanical systems, and stretchable/wearable devices for healthcare applications.